Research Square

Preprints are preliminary reports that have not undergone peer review.
They should not be considered conclusive, used to inform clinical practice,
or referenced by the media as validated information.

Identification and Validation of CCL3 as an Inflammation-Related Biomarker for Arteriovenous Fistula Dysfunction

Xin Li
The 924th Hospital of the Joint Logistics Support Force of the Chinese People's Liberation Army
Shibo Meng
Affiliated Hospital of Guilin Medical University
Disha Zou
Guilin University of Electronic Technology
Junjun Li
Affiliated Hospital of Guilin Medical University
Xinfang Qin
772145607@qq.com
Affiliated Hospital of Guilin Medical University

Research Article

Keywords: Arteriovenous Fistula, Inflammation, C-C Motif Chemokine Ligand 3, Biomarkers, Vascular Remodeling

Posted Date: September 27th, 2026

DOI: https://doi.org/10.21203/rs.3.rs-10992406/v1

License: This work is licensed under a Creative Commons Attribution 4.0 International License.
Read Full License

Additional Declarations: No competing interests reported.

Abstract

Objective

To investigate the key inflammation-related genes associated with arteriovenous fistula (AVF) dysfunction and to identify and validate their associations with AVF dysfunction, thereby providing new directions and a theoretical basis for the prevention, diagnosis, and treatment of AVF dysfunction.

Methods

Bioinformatics analysis and the GeneCards database were used to screen for inflammation-related differentially expressed genes (DEGs) associated with AVF dysfunction, and C-C motif chemokine ligand 3 (CCL3) was identified as a candidate gene. Immune infiltration analysis was performed to explore the association between CCL3 and various immune cell types. Subsequently, CCL3 expression in clinical samples and its relationship with clinical parameters were validated.

Results

(1) A total of 64 inflammation-related DEGs were identified through bioinformatics screening, with CCL3 emerging as a potential key gene associated with AVF dysfunction. (2) Immune infiltration analysis revealed that CCL3 was positively correlated with activated mast cells, monocytes, and neutrophils, and negatively correlated with resting mast cells. (3) Both intimal thickness and the intima-to-media thickness ratio were significantly greater in the AVF dysfunction group compared to the initial AVF group. (4) Immunohistochemical staining showed that CCL3 expression was significantly higher in the AVF dysfunction group than in the control group. Furthermore, CCL3 expression was positively correlated with intimal thickness and the intima-to-media thickness ratio, whereas no significant correlations were observed with clinical parameters such as age, albumin, or hemoglobin.

Conclusion

This study demonstrates that CCL3 is highly expressed in venous tissues of patients with AVF dysfunction, supporting its potential as an inflammation-related biomarker for the diagnosis and management of AVF dysfunction.

Background

According to the Sixth National Survey of Chronic Diseases and Risk Factors in China, the current prevalence of chronic kidney disease (CKD) among Chinese adults is approximately 8.2% [1], and its incidence is increasing steadily. CKD patients frequently present with various severe complications,

including cardiovascular diseases [2, 3], gastrointestinal disorders [4, 5], electrolyte disturbances [6, 7], mineral and bone disorders [8, 9], and hematological diseases [10, 11], resulting in substantial clinical complexity, poor prognosis, and high treatment costs. Consequently, CKD has emerged as a major public health concern that poses a serious threat to human health worldwide. Currently, maintenance hemodialysis (MHD) remains the predominant renal replacement therapy for patients with end-stage renal disease, and establishing safe, functional vascular access is essential for the effective delivery of MHD. The current US Kidney Disease Outcomes Quality Initiative guidelines [12] recommend the native arteriovenous fistula (AVF) as the preferred vascular access for MHD patients, owing to its superior long-term patency, well-established surgical technique, and lower rates of complications and infections. Despite generally favorable patency and maturation rates, a considerable proportion of patients experience AVF maturation disorders, such as stenosis, occlusion, and thrombosis, which compromise dialysis adequacy and may jeopardize patient safety and outcomes [13].

At present, the specific molecular mechanisms underlying AVF dysfunction remain incompletely understood. Vascular intimal hyperplasia and vascular remodeling are widely accepted as the principal contributors to vascular injury and AVF failure [14,15], and are closely associated with pathophysiological events such as inflammation, endothelial damage, and the proliferation and migration of vascular smooth muscle cells [14, 16]. Notably, inflammation is considered a key driver of intimal hyperplasia [17–19]. Existing evidence indicates that surgical trauma, hemodynamic alterations, and the uremic toxin and oxidative stress milieu characteristic of end-stage renal disease can initiate and amplify local inflammatory responses [20]. This inflammatory microenvironment directly acts on resident vascular wall cells, stimulating vascular smooth muscle cell proliferation and migration, activating fibroblasts and promoting vascular fibrosis, promoting oxidative stress, and triggering immune-mediated injury to endothelial cells. Collectively, these effects contribute to the pathological progression of intimal hyperplasia and thrombosis, culminating in vascular luminal dysfunction [21].

Bioinformatics, through the integrative analysis of multi-omics data, including genomics, transcriptomics, and proteomics, elucidates disease characteristics at the molecular level and facilitates disease diagnosis, thereby offering novel directions for mechanistic research and clinical translation [22, 23]. Thus, by leveraging bioinformatics approaches, we can retrieve and curate raw data from public repositories to identify genes specifically up- or down-regulated in diseased tissues and evaluate their potential utility as biomarkers for disease diagnosis, management, and prognostic assessment. Concurrently, functional enrichment analyses of gene sets can be performed to delineate the biological processes (BP) and signaling pathways involved, thereby elucidating the potential molecular mechanisms underlying the disease.

Currently, the GEO database contains transcriptomic data relevant to AVF. Therefore, we posit that a bioinformatics-based exploration of inflammation-related genes and mechanisms in AVF dysfunction among MHD patients is of substantial significance for identifying differential genes and key signaling pathways. In this study, we analyze microarray datasets to screen for pivotal inflammation-related genes

implicated in AVF dysfunction, followed by validation of their expression levels in collected clinical tissue samples, with the aim of providing a theoretical foundation for the discovery of novel therapeutic targets.

Materials and Methods

Data source and identification of differentially expressed genes (DEGs)

In this study, differential expression analysis was performed on the GSE39488 dataset using GEO2R, an online analysis available through the GEO database. Venous tissue specimens from the AVF segments of MHD patients (GSM969946, GSM969949, GSM969950, GSM969951, GSM969952, GSM969953) were assigned to the AVF group, while normal cephalic vein tissue specimens from CKD patients (GSM969945, GSM969947, GSM969948, GSM969954) served as the normal control group. Gene expression differences between the two groups were compared. DEGs with statistical significance were identified using the screening criteria of $|logFC| > 1$ and adjusted p-value < 0.05, after removing duplicates and blank entries.

Acquisition of inflammation-related target genes

The human gene database GeneCards was searched using the keyword “Inflammatory Response” to retrieve inflammation-related genes, with the database updated through September 2024.

Screening of inflammation-related DEGs

Intersection analysis between the DEGs and inflammation-related genes was performed using the online tool Venny 2.1.0 (https://bioinfogp.cnb.csic.es/tools/venny/), yielding inflammation-related differentially expressed genes.

Construction of protein-protein interaction (PPI) network

The inflammation-related DEGs were imported into the STRING database (https://cn.string-db.org/) with the species set to “Homo sapiens” and a highest confidence threshold of 0.4. Isolated nodes without connections were excluded to construct the PPI network. The resulting PPI data were imported into Cytoscape 3.10.0, and the CytoNCA 2.2 plugin was used to identify core genes.

Enrichment analysis

Kyoto Encyclopedia of Genes and Genomes (KEGG) pathway and Gene Ontology enrichment analyses of the inflammation-related DEGs were performed using the DAVID database (https://david.ncifcrf.gov/),

with a significance threshold of $p < 0.05$. Visualization was carried out using the Bioinformatics Platform (https://www.bioinformatics.com.cn/).

Immune infiltration analysis

Immune infiltration analysis of the GSE39488 dataset was performed using the CIBERSORT package in R to compare immune cell type composition between the two groups, thereby assessing differences in immune cell infiltration. Subsequently, a correlation analysis was performed between the key genes and each immune cell type to further elucidate their relationships with immune responses [24].

Study subjects

Discarded venous tissues were collected from patients who underwent initial AVF creation for MHD or AVF revision for AVF dysfunction at the Department of Nephrology, First Affiliated Hospital of Guilin Medical University, between October 2024 and February 2026. Discarded venous tissues from CKD patients undergoing initial AVF creation surgery served as controls. All participants provided written informed consent. The collection and use of tissue specimens were approved by the Ethics Committee of the First Affiliated Hospital of Guilin Medical University (approval No. 2024YJSLL-34).

Inclusion criteria

(1) CKD patients who underwent initial AVF creation for MHD therapy or patients who underwent AVF revision due to AVF dysfunction at the Department of Nephrology, First Affiliated Hospital of Guilin Medical University, between October 2024 and February 2026; (2) age > 18 years; (3) all surgical procedures were performed by two surgeons with at least 3 years of AVF surgical experience and more than 100 related cases; (4) the surgical approach involved end-to-side anastomosis of the cephalic vein at the wrist to the radial artery; (5) all patients voluntarily participated in the study and provided written informed consent.

Exclusion criteria

(1) Concomitant malignancy (including solid tumors and hematological malignancies), autoimmune diseases, severe infections, or fever of unknown origin; (2) an end-to-end or side-to-side anastomosis was performed; (3) gastrointestinal bleeding, major trauma, or severe cardiovascular or cerebrovascular events within 1 month before enrollment; (4) use of corticosteroids or immunosuppressive agents within the preceding year.

Collection of clinical data of study subjects

(1) General preoperative inpatient data were collected for each group, including age, sex, smoking history, and histories of diabetes mellitus and hypertension.

(2) Clinical laboratory data were collected on the day after admission and before surgery, including: red blood cell count, white blood cell count, hemoglobin, platelet count, absolute lymphocyte count, absolute neutrophil count, phosphorus, calcium, potassium, thrombin time, D-dimer, activated partial thromboplastin time, fibrinogen, albumin, serum total cholesterol, serum high-density lipoprotein, serum low-density lipoprotein, and serum triglycerides. The platelet-to-lymphocyte ratio and neutrophil-to-lymphocyte ratio were subsequently calculated. All laboratory measurements were performed by the hospital's Department of Clinical Laboratory.

Experimental grouping

Owing to ethical constraints and the specific nature of clinical practice, it was not feasible to collect paired venous tissue samples from the same patient at both initial AVF creation and subsequent revision, nor was it possible to obtain normal venous tissue adjacent to the lesion from patients with AVF dysfunction as controls. Therefore, this study included tissue samples from different patients for comparison. Although inter-individual differences in genetic and clinical backgrounds may exist, the study was designed to minimize the influence of individual variability through rigorous statistical adjustment, thereby identifying potential universal biomarkers associated with AVF dysfunction.

Experimental group: Patients undergoing AVF revision due to AVF dysfunction. Two segments of discarded stenotic venous tissue, each approximately 0.5 cm in length, were collected intraoperatively.

Control group: CKD patients undergoing initial AVF creation for MHD therapy at our hospital. Two segments of discarded normal venous tissue, each approximately 0.5 cm in length, were collected intraoperatively.

Main reagents

Rabbit recombinant monoclonal antibody against C-C motif chemokine ligand 3 (CCL3; clone EPR23751-54, Abcam, UK) and rabbit secondary antibody (Zhongshan Golden Bridge Biotechnology, Beijing, China).

Hematoxylin-eosin staining of vascular tissues

Venous tissues were fixed within 30 minutes after excision. Prior to fixation, the tissue surface was rinsed with normal saline to remove blood and debris, then the tissue was immersed in neutral formalin solution and stored at 4°C for approximately 24 hours. Following fixation, specimens were rinsed, dehydrated in graded alcohols, cleared, infiltrated with paraffin, and embedded. Paraffin blocks were sectioned at a thickness of 5 μm using a microtome, and hematoxylin-eosin staining was performed according to standard protocols to evaluate the morphological structure of the vascular intima and media. Morphometric measurements were performed using CaseViewer image software. For each section, three non-overlapping high-power fields were randomly selected, avoiding areas of calcification, necrosis, or incomplete intimal architecture. Intimal thickness, medial thickness, and the intima-to-media thickness ratio were measured. The average values from the three fields were calculated as the

representative value for each section. The measurements were defined as follows: intimal thickness was defined as the perpendicular distance from the luminal surface to the inner aspect of the internal elastic lamina, while medial thickness was defined as the perpendicular distance from the outer aspect of the internal elastic lamina to the inner aspect of the external elastic lamina.

Immunohistochemical staining of vascular tissues

After deparaffinization and rehydration, paraffin sections underwent antigen retrieval in ethylenediaminetetraacetic acid at high pressure for 9 minutes, followed by blocking of endogenous peroxidase activity and blocking with serum. Sections were sequentially incubated with CCL3 primary antibody (diluted 1:500) and rabbit secondary antibody, then developed, counterstained, differentiated, blued, dehydrated, cleared, and coverslipped. Brownish-yellow staining was considered positive. For each section, three non-overlapping high-power fields were randomly selected, and the mean optical density (calculated as integrated optical density/area) was calculated using ImageJ software. The mean optical density averaged across the three fields was taken as the relative protein expression level of the specimen.

Statistical analysis

Statistical analyses were performed using IBM SPSS Statistics 26.0. Continuous data were tested for normality; normally distributed data were expressed as mean ± standard deviation ($\bar{x} \pm s$) and compared between groups using independent samples *t*-tests, while non-normally distributed data were expressed as median (lower quartile, upper quartile) (M [P25, P75]) and compared using the Mann-Whitney U test. Categorical data were expressed as counts (percentages) (n [%]) and compared using the chi-square test. Correlation analysis between CCL3 and clinical parameters was performed using the Pearson correlation coefficient for normally distributed data and the Spearman rank correlation coefficient for non-normally distributed data. Graphs were generated using GraphPad Prism 10.1.2. All hypothesis tests were two-sided, and a P value < 0.05 was considered statistically significant.

Results

Screening and visualization of inflammation-related DEGs

In this study, after batch correction and normalization of the GSE39488 dataset, 97 statistically significant DEGs were identified, comprising 74 upregulated and 23 downregulated genes. These DEGs were visualized as a volcano plot (Fig. 1A). A search of the GeneCards database for targets closely associated with the inflammatory response yielded 17,405 related genes. Using the Venny 2.1.0 platform, the intersection of the above DEGs and inflammation-related targets was determined, ultimately yielding 64 inflammation-related DEGs (Fig. 1B).

(A)DEGs volcano plot (upregulated genes: 74, downregulated genes: 23).(B) Intersection diagram of DEGs and genes targeting inflammatory responses(Blue indicates DEGs, and yellow denotes inflammation-related targets).(C)Seven core targets.(D)GO results of three ontologies.(E)Pathway

Analysis.(F)Differences in the infiltration of various immune cells between the two groups.(G)The correlation between CCL3 and the infiltration of various immune cells.

Construction of the PPI network for inflammation-related DEGs

The 64 inflammation-related DEGs were imported into the STRING database to construct a PPI network, which, after applying the filtering criteria, comprised 64 nodes and 99 edges. The PPI data were then imported into Cytoscape 3.10.0, and the CytoNCA plugin was used to calculate the average values of degree, betweenness, closeness, eigenvector centrality, and local average connectivity (LAC). Nodes with values above the respective average thresholds were retained, yielding seven core target genes, including CCL3, C-X-C motif chemokine receptor 4 (CXCR4), and early growth response 1 (EGR1), among others (Table 1 and Fig. 1C).

Table 1
Topological parameters of the seven core targets

Gene	Betweenness	Closeness	Degree	Eigenvector	LAC
EGR1	126.5714286	0.591836735	13	0.293143839	5.846154
NR4A2	123.8238095	0.568627451	13	0.300950527	6.153846
FOS	109.5253968	0.644444444	16	0.364173084	7.500000
CCL3	65.27142857	0.500000000	9	0.196873263	4.222222
CXCR4	60.44603175	0.517857143	9	0.159035355	3.333333
NR4A1	59.81904762	0.527272727	10	0.259541869	6.400000
CD69	47.80634921	0.508771793	10	0.216029242	4.400000

Enrichment analysis results

Using the DAVID database to analyze the 64 inflammation-related DEGs, the genes were found to be involved in 546 BPs, 55 molecular functions, eight cellular components, and 20 signaling pathways (Figs. 1D-E).

Screening of key genes

Genes involved in the most significantly enriched pathway, the cytokine-cytokine receptor interaction pathway, identified by KEGG enrichment analysis (namely INHBA, TNFRSF12A, CCL4, CXCR4, TNFRSF11B, CCL3, and IL1RL1) were cross-referenced with the seven core target genes identified by the PPI network in section 2.2 (CCL3, CXCR4, EGR1, FOS, NR4A1, NR4A2, and CD69). This analysis yielded two overlapping genes: CCL3 and CXCR4. Furthermore, within the PPI network, CCL3 exhibited higher betweenness (65.27), eigenvector centrality (0.197), and LAC (4.22) than CXCR4 (betweenness, 60.45; eigenvector, 0.159; LAC, 3.33), indicating that CCL3 not only occupies a central regulatory position but is

also closely connected with transcriptional regulatory hubs (FOS, EGR1), suggesting strong functional synergy and network robustness. These topological features suggest that CCL3 may serve as a key gene linking upstream transcriptional regulation with downstream inflammatory effects.

Immune infiltration analysis and correlation analysis between key genes and immune cells

The immunological characteristics of the GSE39488 dataset were evaluated for immune cell infiltration, revealing a significant difference in the proportion of resting mast cells between AVF venous tissues and normal cephalic vein tissues (Fig. 1F). The expression level of CCL3 was positively correlated with the infiltration proportions of activated mast cells, monocytes, and neutrophils, while being negatively correlated with resting mast cells (Fig. 1G).

Comparison of preoperative clinical data between study groups

Owing to limitations in the study period, enrollment difficulties, and the availability of clinical cases, a total of 24 subjects were ultimately included in this study: 12 patients undergoing initial AVF creation for MHD therapy at our hospital and 12 patients undergoing AVF revision due to AVF dysfunction. There were no statistically significant differences between the two groups in age, albumin, hemoglobin, or other parameters, as detailed in Table 2.

Table 2
Comparison of clinical data between the first-time AVF group and the AVF dysfunction group of patients

Characteristics	Initial AVF group (n = 12)	AVF dysfunction group (n = 12)	$x^2/t/Z$	*P*
Gender,n(%)			0.178	0.673
Male	7(58.33)	8(66.67)		
Female	5(41.67)	4(33.33)		
Smoking history,n(%)			0.168	0.682
yes	6(50.00)	7(58.33)		
no	6(50.00)	5(41.67)		
Diabetes history,n(%)			2.274	0.132
yes	4(33.33)	1(8.33)		
no	8(66.67)	11(91.67)		
Hypertension history,n(%)			0.253	0.615
yes	9(75.00)	10(83.33)		
no	3(25.00)	2(16.67)		
Age,(years)	60.75 ± 13.59	54.92 ± 14.90	1.002	0.327
Red blood cell count(10^{12}/L)	3.135(2.7,3.7)	3.305(2.9,4.5)	-0.635	0.525
White blood cell count(10^9/L)	7.43 ± 2.21	7.01 ± 2.96	0.392	0.699
Hemoglobin(g/L)	97.75 ± 17.56	106.25 ± 15.70	-1.250	0.224
Platelets(10^9/L)	221.83 ± 67.42	195.83 ± 85.05	0.830	0.416
Absolute value of neutrophils(×10^9/L)	5.25 ± 1.91	4.92 ± 3.06	0.317	0.754
Absolute value of lymphocytes(×10^9/L)	1.166(0.7,1.8)	0.859(0.6,1.3)	-1.039	0.299
Absolute value of monocytes(×10^9/L)	0.631(0.3,0.9)	0.461(0.4,0.7)	-0.837	0.402
Neutrophil/lymphocyte ratio	5.094(3.1,6.2)	3.768(3.2,4.9)	-0.808	0.419
Platelet/lymphocyte ratio	169.508(108.7,317.9)	192.281(120.8,329.7)	-0.058	0.954
C-reactive protein(mg/L)	7.04 ± 4.71	5.29 ± 4.42	0.938	0.359

Characteristics	Initial AVF group	AVF dysfunction group	$x^2/t/Z$	P
	(n = 12)	(n = 12)		
Albumin(g/L)	37.80(35.9,40.8)	39.60(37.9,40.8)	-0.664	0.507
D-dimer(mg/L)	0.885(0.6,2.9)	1.520(0.7,2.5)	-0.029	0.977
Thrombin time(s)	18.32 ± 1.45	18.31 ± 1.59	0.013	0.989
Fibrinogen(g/L)	3.42 ± 1.27	3.13 ± 1.02	0.631	0.534
Activation of partial thromboplastin time(s)	29.60(27.40,31.80)	27.60(25.10,29.10)	1.299	0.207
Phosphorus(mmol/L)	1.87 ± 0.63	1.95 ± 0.77	-0.290	0.775
Calcium(mmol/L)	1.90 ± 0.40	2.11 ± 0.21	-1.690	0.105
Potassium(mmol/L)	4.86 ± 1.27	4.48 ± 1.01	0.815	0.424
Triglyceride(mmol/L)	1.370(1.0,2.4)	1.180(0.6,1.7)	-1.328	0.184
High-density lipoprotein(mmol/L)	0.925(0.7,1.2)	1.095(1.0,1.2)	-1.127	0.260
Low-density lipoprotein(mmol/L)	2.13 ± 1.04	1.66 ± 0.45	1.436	0.172

Hematoxylin and eosin staining

Light microscopy revealed varying degrees of intimal hyperplasia in the venous segments of the AVF dysfunction group (Fig. 2A). Both intimal thickness and the intima-to-media thickness ratio in the AVF dysfunction group were significantly greater than those in the initial AVF group ($P < 0.05$) (Table 3).

Table 3
Comparison of intima, media, and intima/media ratio between the first-time AVF group and the AVF dysfunction group

Characteristics	Initial AVF group(n = 12)	AVF dysfunction group(n = 12)	t/Z	P
intimal thickness(μm)	27.50(19.17,40.75)	145.00(68.17,676.00)	-3.985	< 0.001
media thickness(μm)	223.67(141.75,277.75)	238.00(146.67,282.83)	-0.462	0.671
intimal-to-medial thickness ratio	0.13(0.10,0.15)	0.75(0.43, 2.41)	-4.041	< 0.001

Immunohistochemical detection of CCL3 protein expression in vascular tissues

Immunohistochemical staining was performed to detect CCL3 protein expression in vascular tissues. The staining results showed that CCL3 was predominantly expressed in the cytoplasm of endothelial cells and vascular smooth muscle cells. Compared with the control group, the AVF dysfunction group exhibited significantly higher CCL3 expression ($P < 0.05$; Figs. 2B-C).

Correlation analysis between biomarker levels and clinical parameters

To further explore the role of CCL3 in patients with chronic renal failure, we performed correlation analyses between CCL3 protein expression levels in tissue samples and clinical data. The results demonstrated that CCL3 expression was positively correlated with intimal thickness and the intima-to-media thickness ratio, whereas no significant correlations were observed with age, albumin, hemoglobin, or other clinical parameters in these patients (Tables 4).

Table 4
The correlation between CCL3 protein levels and clinical indicators in patients with chronic renal failure

Characteristics	***r***	***P***
intimal thickness(μm)	0.640	0.001
media thickness(μm)	-0.053	0.806
intimal-to-medial thickness ratio	0.660	< 0.001
Age,(years)	-0.190	0.374
White blood cell count(10^9/L)	0.148	0.491
Red blood cell count(10^{12}/L)	0.345	0.098
Hemoglobin (g/L)	0.201	0.347
Platelets (10^9/L)	0.079	0.713
Absolute value of neutrophils (×10⁹/L)	0.107	0.619
Absolute value of lymphocytes (×10⁹/L)	-0.001	0.997
Absolute value of monocytes (×10⁹/L)	-0.141	0.511
Neutrophil/lymphocyte ratio	-0.253	0.233
Platelet/lymphocyte ratio	-0.143	0.506
C-reactive protein(mg/L)	0.170	0.427
Albumin(g/L)	0.042	0.052
D-dimer(mg/L)	0.102	0.635
Thrombin time(s)	-0.090	0.676
Fibrinogen(g/L)	0.097	0.652
Activation of partial thromboplastin time(s)	-0.310	0.141
Phosphorus(mmol/L)	0.080	0.710
Calcium(mmol/L)	0.111	0.604
Potassium(mmol/L)	-0.092	0.669
Triglyceride(mmol/L)	-0.184	0.391
High-density lipoprotein(mmol/L)	0.208	0.331
Low-density lipoprotein(mmol/L)	-0.218	0.306

Discussion

AVF dysfunction is a clinical state in which the AVF fails to provide adequate dialysis due to diminished blood flow or access occlusion resulting from various causes, including maturation failure, vascular stenosis, thrombosis, and calcification. The underlying mechanisms involve complex interactions among intimal hyperplasia, vascular calcification, hemodynamic alterations, inflammatory responses, and thrombosis [25, 26]. It is characterized by a cascade of upstream and downstream events: upstream events include endothelial dysfunction and vascular smooth muscle cell injury caused by repeated puncture or balloon angioplasty, the uremic milieu, and hemodynamic changes following AVF creation, whereas downstream events refer to the biological vascular responses to these upstream stimuli, encompassing oxidative stress, inflammation, and the proliferation and migration of endothelial and smooth muscle cells [27]. Although current surgical techniques for AVF creation, endovascular interventions, and dialysis cannulation methods continue to improve, these approaches have not fully prevented AVF dysfunction or postoperative recurrence of access failure. Therefore, in-depth investigation into the relevant mechanisms is important for improving long-term AVF patency and patients' quality of life.

Previous studies have largely focused on single-factor analyses, an approach that cannot systematically elucidate the complex mechanisms underlying AVF dysfunction. In recent years, with the continued advancement of high-throughput sequencing technologies, bioinformatics has been increasingly applied to medical research, offering new opportunities to explore the molecular mechanisms underlying AVF dysfunction. In the study of AVF dysfunction, bioinformatics enables the integration and analysis of large-scale gene expression and proteomic data, thereby facilitating a more systematic elucidation of the molecular mechanisms underlying AVF dysfunction and aiding in the identification of potential diagnostic biomarkers and therapeutic targets. For instance, Lu P et al. [28] used high-throughput microarray data, combined with immunohistochemistry and Western blotting, to validate the expression levels of key immune-related genes and systematically analyzed their roles and immune cell infiltration in AVF maturation from a bioinformatics perspective. Similarly, Martinez L et al. [29] performed high-throughput sequencing on AVF failing tissues and normal vein tissues, integrating reverse transcription quantitative polymerase chain reaction, proteomics, and biological network analysis, and identified S100A9, CSF3R, S100A8, VNN2, and FPR1 as predominantly expressed in vascular smooth muscle cells and associated with AVF maturation failure. Notably, the expression levels of S100A8 and S100A9 were positively correlated with the degree of postoperative intimal hyperplasia and the product of medial fibrosis and intimal hyperplasia. These findings underscore the significant value of bioinformatics in investigating the mechanisms of AVF dysfunction and provide a solid foundation for further exploration.

Summary of research findings

Given the current state of research on AVF dysfunction, no universally accepted biomarker or model for accurately predicting AVF dysfunction has been established to date. We therefore used this knowledge

gap as the basis for our study and performed differential gene expression analysis of transcriptomic data from AVF venous tissue specimens of MHD patients and normal cephalic vein tissue specimens of CKD patients in the GSE39488 dataset, identifying 97 DEGs, 64 of which were inflammation-related. Using the STRING database and Cytoscape 3.10.0, we identified seven core target genes: CCL3, CXCR4, EGR1, FOS, NR4A1, NR4A2, and CD69.

Subsequent bioinformatics analysis of the 64 inflammation-related DEGs using the DAVID online database revealed that these genes were predominantly enriched in BP such as chemotaxis regulation, skeletal muscle cell differentiation, and negative regulation of cell-matrix adhesion. Cellular component enrichment analysis indicated that these genes were mainly localized to transcriptional regulatory complexes, the external side of the plasma membrane, and platelet alpha granule lumen. Molecular function analysis showed that the related genes are primarily involved in RNA polymerase II-specific DNA-binding transcription factor binding, DNA-binding transcription factor binding, and glucocorticoid receptor binding. These results strongly suggest that the 64 inflammation-related DEGs do not act as isolated effector molecules but rather function within a coordinated transcriptional regulatory network, playing central roles in gene expression. Dysregulation of these functions may promote vascular smooth muscle cell migration, proliferation, and inflammation, thereby accelerating intimal hyperplasia or vascular stenosis, and may provide a molecular basis for the progressive nature of AVF dysfunction [30, 31].

KEGG pathway analysis revealed that the 64 inflammation-related DEGs were mainly involved in the cytokine-cytokine receptor interaction pathway [32–34], the p53 signaling pathway [35], the TGF-β signaling pathway [36, 37], and the Toll-like receptor signaling pathway [18, 38, 39], among others, which may contribute to the pathological process of AVF-associated vascular remodeling. This is consistent with previous reports on the pathogenesis of AVF maturation failure. Among these, the cytokine-cytokine receptor interaction pathway showed the greatest enrichment. Previous studies have established that this pathway serves as a central hub connecting initial vascular injury signals to subsequent pathological remodeling: following vascular intervention or injury, the pathway is rapidly activated, driving intimal hyperplasia and luminal stenosis through three key mechanisms: recruitment and activation of inflammatory cells, phenotypic switching, proliferation and migration of smooth muscle cells, and extracellular matrix remodeling and fibrosis. Therefore, we postulate that the cytokine-cytokine receptor interaction signaling pathways play a critical role in AVF dysfunction.

By cross-referencing the cytokine-cytokine receptor interaction pathway genes from the KEGG enrichment analysis with the seven core target genes identified through STRING and Cytoscape 3.10.0 screening, and integrating network topological feature analysis, we found that CCL3 occupies a central regulatory position and is closely connected to the transcriptional regulatory hubs FOS and EGR1, exhibiting strong functional synergy and network robustness. This suggests that CCL3 may be a key gene linking upstream transcriptional regulation to downstream inflammatory effects.

Relationship between CCL3 and AVF dysfunction

Building upon the bioinformatics screening results and existing literature, we observed that extensive studies have confirmed that CCL3, as an inflammatory chemokine, may participate in pathophysiological processes such as tissue repair, angiogenesis, and thrombosis by regulating inflammatory responses, immune cell migration, and vascular smooth muscle cell functions, thereby promoting intimal hyperplasia and vascular stenosis and ultimately leading to vascular dysfunction. However, no study to date has examined CCL3 expression in AVF dysfunction or its association with intimal hyperplasia. To further validate the role of CCL3 in AVF dysfunction, we performed immunohistochemical staining on clinical samples from our center and confirmed that CCL3 expression was upregulated in tissues from patients with AVF dysfunction ($P < 0.05$), consistent with the database analysis results.

Current evidence indicates that CCL3 is an important chemokine produced by immune cells, including monocytes [40] and lymphocytes [41], and that it can recruit macrophages [42] and neutrophils [43] to inflammatory sites. Related studies have shown that CCL3 mediates mast cell degranulation, thereby impairing endothelial function [40, 44]; it also promotes the migration of CD14 + CD16+ monocyte subsets, exacerbating local inflammation, whereas blockade of the CCL3/CCR1 signaling axis significantly inhibits monocyte infiltration and attenuates vascular inflammation [40]. Under acute inflammatory conditions, upregulated CCL3 expression promotes neutrophil trafficking to atherosclerotic plaques, thus accelerating atherosclerosis and vascular stenosis [45]. In chronic inflammatory diseases, CCL3 facilitates the migration of inflammatory cells into synovial and vascular tissues, and is closely associated with neovascularization and tissue hyperplasia [46]. Other studies have indicated that CCL3 regulates miR-374b expression through the JNK, ERK, and p38 signaling pathways; CCL3 upregulation suppresses miR-374b expression, thereby relieving inhibition of vascular endothelial growth factor A and increasing its expression, which promotes neovascularization. Aberrant neovascularization not only aggravates local inflammation and extracellular matrix remodeling but also promotes vascular smooth muscle cell migration and proliferation, further driving intimal thickening and luminal narrowing [47]. Our results demonstrated that CCL3 expression in vascular tissues was significantly higher in the AVF dysfunction group than in the initial AVF group. Based on these findings, we hypothesize that CCL3 overexpression may participate in the pathological progression of AVF dysfunction by mediating inflammatory cell infiltration, activating local inflammatory responses, and regulating vascular smooth muscle cell proliferation, migration, and extracellular matrix remodeling, thereby providing new directions for research into immune-based biomarkers and targeted therapies for AVF dysfunction.

Further studies have revealed that CCL3 is also closely associated with thrombosis [48, 49]. Luo X et al. [50], through single-cell transcriptomic analysis, found that CCL3 can promote excessive immune system activation and facilitate microthrombus formation. Vascular thrombosis in turn induces local inflammation, abnormal shear stress and turbulent flow, and endothelial injury, triggering vascular smooth muscle cell proliferation and migration, leading to luminal stenosis and consequent vascular dysfunction [51]. Therefore, based on these findings, we speculate that CCL3 may indirectly exacerbate AVF dysfunction by promoting thrombosis, further supporting its potential biological relevance.

Moreover, Sun H et al. [52] demonstrated that platelet-derived CCL3 can cause vascular injury through the CCL3/CCR5 signaling pathway by affecting endothelial cell mitochondrial dysfunction, and both in vivo and in vitro experiments revealed that CCL3 inhibition significantly suppressed cell proliferation and migration, whereas CCL3 overexpression promoted these processes [53]. Collectively, these observations indicate that CCL3 may play an important role in the initiation and progression of AVF dysfunction.

In summary, CCL3 may promote intimal hyperplasia and luminal stenosis, ultimately leading to AVF dysfunction, through mechanisms involving the regulation of inflammatory responses, vascular smooth muscle cell proliferation and migration, thrombosis, and immune cell infiltration. Furthermore, immune infiltration analysis revealed associations between CCL3 and multiple immune cell subsets, suggesting that CCL3 may contribute to AVF intimal hyperplasia by regulating inflammatory cells and mast cells. These findings provide a novel theoretical basis for understanding the molecular mechanisms underlying AVF dysfunction and suggest that CCL3 may serve as a biomarker for predicting AVF dysfunction and as a potential target for therapeutic intervention.

Limitations and future perspectives

Although this study provides valuable insights into the molecular mechanisms and immune infiltration characteristics of AVF dysfunction, several limitations should be acknowledged. First, this is a single-center, small-sample exploratory study with a relatively limited overall sample size, and the results may only reflect the features of AVF dysfunction patients at this center or in this region. Additionally, due to ethical constraints and the specific nature of clinical practice, we were unable to collect paired venous tissue samples from the same patient at both the initial AVF creation and revision surgeries, nor could we obtain normal venous tissues adjacent to the lesion from patients with AVF dysfunction as controls. Furthermore, this study measured CCL3 expression only in venous tissues, did not assess immune cell infiltration, and did not include in vitro cellular or in vivo animal experiments for mechanistic validation. Moreover, the AVF dysfunction group may have been affected by confounding factors such as long-term dialysis, shear-stress injury, and chronic inflammation, making it difficult to fully isolate the independent effect of CCL3 overexpression. Future multicenter, large-sample clinical studies are warranted, along with animal models of targeted CCL3 silencing/overexpression and in vitro functional experiments using vascular smooth muscle cells and endothelial cells, to further validate the regulatory mechanisms and clinical predictive value of CCL3 in AVF stenosis, thereby providing experimental evidence for early intervention and targeted therapy of AVF dysfunction.

Conclusion

This study demonstrates that CCL3 is highly expressed in venous tissues from patients with AVF dysfunction, suggesting that CCL3 may serve as a biomarker for the diagnosis and management of AVF dysfunction.

Abbreviations

AVF
Arteriovenous Fistula
BP
Biological Process
CC
Cellular Component
CCL3
C-C Motif Chemokine Ligand 3
CD69
Cluster of Differentiation 69
CKD
Chronic Kidney Disease
CXCR4
C-X-C Motif Chemokine Receptor 4
EGR1
Early Growth Response 1
ESRD
End-Stage Renal Disease
FOS
FBJ Murine Osteosarcoma Viral Oncogene Homolog
GO
Gene Ontology
HE
Hematoxylin-Eosin
KEGG
Kyoto Encyclopedia of Genes and Genomes
MF
Molecular Function
MHD
Maintenance Hemodialysis
NLR
Neutrophil/Lymphocyte Ratio
NR4A1
Nuclear Receptor Subfamily 4 Group A Member 1
NR4A2
Nuclear Receptor Subfamily 4 Group A Member 2
PLR
Platelet/Lymphocyte Ratio

PPI
Protein-Protein Interaction

Declarations

Consent for publication

All authors have agreed to the submission and publication of this manuscript.

Competing interests

The authors declare that they have no known competing financial interests or personal relationships that could have appeared to influence the work reported in this paper.

Ethics approval and consent to participate

All procedures involving human subjects and human specimens in this study were conducted in accordance with the Declaration of Helsinki and were approved by the Ethics Committee of the First Affiliated Hospital of Guilin Medical University (Ethical Approval Number: 2024YJSLL-34). Written informed consent was obtained from all patients prior to their participation in the study.

Funding

This work was supported by the Guangxi Natural Science Foundation (Grant No. 2026GXNSFHA00640324) and the Guilin Municipal Self-funded Science and Technology Plan Project (Grant No. 20250144z).

Author Contribution

Xin Li and Shibo Meng performed the experiments and wrote the manuscript; Disha Zou designed the experiments and analyzed the data; Junjun Li collected the data; Xinfang Qin interpreted the data and revised the manuscript.

Acknowledgement

We sincerely thank Elsevier Research & Academic for providing analytical support.

Availability of data and materials

The data presented in this study are available from the corresponding author upon reasonable request.

References

1. Wang L, Xu X, Zhang M, Hu C, Zhang X, Li C, Nie S, Huang Z, Zhao Z, Hou FF, Zhou M. Prevalence of Chronic Kidney Disease in China: Results From the Sixth China Chronic Disease and Risk Factor Surveillance. JAMA Intern Med. 2023;183(4):298–310.
2. Marx-Schütt K, Cherney DZI, Jankowski J, Matsushita K, Nardone M, Marx N. Cardiovascular disease in chronic kidney disease. Eur Heart J. 2025;46(23):2148–60.
3. Matsushita K, Ballew SH, Wang AY, Kalyesubula R, Schaeffner E, Agarwal R. Epidemiology and risk of cardiovascular disease in populations with chronic kidney disease. Nat Rev Nephrol. 2022;18(11):696–707.
4. Lin Y, Li C, Waters D, Kwok CS. Gastrointestinal bleeding in chronic kidney disease patients: a systematic review and meta-analysis. Ren Fail. 2023;45(2):2276908.
5. Biruete A, Shin A, Kistler BM, Moe SM. Feeling gutted in chronic kidney disease (CKD): Gastrointestinal disorders and therapies to improve gastrointestinal health in individuals CKD, including those undergoing dialysis. Semin Dial. 2024;37(4):334–49.
6. Zaslow SJ, Oliveira-Paula GH, Chen W. Magnesium and Vascular Calcification in Chronic Kidney Disease: Current Insights. Int J Mol Sci. 2024;25(2):1155.
7. Dhondup T, Qian Q. Electrolyte and Acid-Base Disorders in Chronic Kidney Disease and End-Stage Kidney Failure. Blood Purif. 2017;43(1–3):179–88.
8. Hu L, Napoletano A, Provenzano M, Garofalo C, Bini C, Comai G, La Manna G. Mineral Bone Disorders in Kidney Disease Patients: The Ever-Current Topic. Int J Mol Sci Int J Mol Sci. 2022;23(20):12223.
9. Yamamoto S, Fukagawa M. Uremic Toxicity and Bone in CKD. J Nephrol. 2017;30(5):623–7.
10. Babitt JL, Lin HY. Mechanisms of anemia in CKD. J Am Soc Nephrol. 2012;23(10):1631–4.
11. Batchelor EK, Kapitsinou P, Pergola PE, Kovesdy CP, Jalal DI. Iron Deficiency in Chronic Kidney Disease: Updates on Pathophysiology, Diagnosis, and Treatment. J Am Soc Nephrol. 2020;31(3):456–68.
12. Lok CE, Huber TS, Lee T, Shenoy S, Yevzlin AS, Abreo K, Allon M, Asif A, Astor BC, Glickman MH, Graham J, Moist LM, Rajan DK, Roberts C, Vachharajani TJ, Valentini RP. National Kidney Foundation. KDOQI Clinical Practice Guideline for Vascular Access: 2019 Update. Am J Kidney Dis. 2020;75(4 Suppl 2):S1–164.
13. Azeem SM, Ehsan O, Khan MI. Patency and Complications of Arterio-venous Fistula Created in Pre- and Post-dialysis Settings. J Coll Physicians Surg Pak. 2022;32(4):510–3.
14. Lee T, Roy-Chaudhury P. Advances and new frontiers in the pathophysiology of venous neointimal hyperplasia and dialysis access stenosis. Adv Chronic Kidney Dis. 2009;16(5):329–38.
15. Yoshizumi M, Abe J, Tsuchiya K, Berk BC, Tamaki T. Stress and vascular responses: atheroprotective effect of laminar fluid shear stress in endothelial cells: possible role of mitogen-activated protein kinases. J Pharmacol Sci. 2003;91(3):172–6.

16. Jiang Y, Qian HY. Transcription factors: key regulatory targets of vascular smooth muscle cell in atherosclerosis. Mol Med. 2023;29(1):2.
17. Shih YC, Chen PY, Ko TM, Huang PH, Ma H, Tarng DC. MMP-9 Deletion Attenuates Arteriovenous Fistula Neointima through Reduced Perioperative Vascular Inflammation. Int J Mol Sci. 2021;22(11):5448.
18. Xie T, Xu Y, Ji L, Sui X, Zhang A, Zhang Y, Chen J. Heme Oxygenase 1/Peroxisome Proliferator-Activated Receptor Gamma Pathway Protects Intimal Hyperplasia and Mitigates Arteriovenous Fistula Dysfunction by Regulating Oxidative Stress and Inflammatory Response. Cardiovasc Ther. 2022;2022:7576388.
19. Wasse H, Huang R, Naqvi N, Smith E, Wang D, Husain A. Inflammation, oxidation and venous neointimal hyperplasia precede vascular injury from AVF creation in CKD patients. J Vasc Access. 2012;13(2):168–74.
20. Shiu YT, Northrup H, Huang Y, Cho ME, Bunsawat K. Cellular and molecular mechanisms underlying hemodialysis arteriovenous fistula dysfunction and approaches to promote maturation: a vascular perspective. Am J Physiol Heart Circ Physiol. 2025;329(1):H241–57.
21. Rai V, Singh H, Agrawal DK. Targeting the Crosstalk of Immune Response and Vascular Smooth Muscle Cells Phenotype Switch for Arteriovenous Fistula Maturation. Int J Mol Sci. 2022;23(19):12012.
22. Jiang P, Sinha S, Aldape K, Hannenhalli S, Sahinalp C, Ruppin E. Big data in basic and translational cancer research. Nat Rev Cancer. 2022;22(11):625–39.
23. Phillips KA. Assessing the Value of Next-Generation Sequencing Technologies: An Introduction. Value Health. 2018;21(9):1031–2.
24. Newman AM, Liu CL, Green MR, Gentles AJ, Feng W, Xu Y, Hoang CD, Diehn M, Alizadeh AA. Robust enumeration of cell subsets from tissue expression profiles. Nat Methods. 2015;12(5):453–7.
25. Wang Y, Qin Y, Huang X, Liu W. MSCTA imaging analysis of autologous arteriovenous fistula dysfunction in maintenance hemodialysis patients. Am J Transl Res. 2024;16(3):955–63.
26. Voorzaat BM, Janmaat CJ, van der Bogt KEA, Dekker FW, Rotmans JI. Patency Outcomes of Arteriovenous Fistulas and Grafts for Hemodialysis Access: A Trade-Off between Nonmaturation and Long-Term Complications. Kidney360. 2020;1(9):916–24.
27. Hu K, Guo Y, Li Y, Lu C, Cai C, Zhou S, Ke Z, Li Y, Wang W. Oxidative stress: An essential factor in the process of arteriovenous fistula failure. Front Cardiovasc Med. 2022;9:984472.
28. Lu P, Wang T, Wan Z, Wang M, Zhou Y, He Z, Liao S, Liu H, Shu C. Immune-Related Genes and Immune Cell Infiltration Characterize the Maturation Status of Arteriovenous Fistulas: An Integrative Bioinformatics Study and Experimental Validation Based on Transcriptome Sequencing. J Inflamm Res. 2024;17:137–52.
29. Martinez L, Tabbara M, Duque JC, Selman G, Falcon NS, Paez A, Griswold AJ, Ramos-Echazabal G, Hernandez DR, Velazquez OC, Salman LH, Vazquez-Padron RI. Transcriptomics of Human

Arteriovenous Fistula Failure: Genes Associated With Nonmaturation. Am J Kidney Dis. 2019;74(1):73–81.

30. Zhao Y, Li Z, Ma H, Pan Z, Cai B, Zhang C, Jiao J. METTL3-Mediated m6A mRNA Modification Facilitates Neointimal Hyperplasia in Arteriovenous Fistula. Arterioscler Thromb Vasc Biol. 2025;45(7):1124–44.
31. Osman I, Dong K, Kang X, Yu L, Xu F, Ahmed ASI, He X, Shen J, Hu G, Zhang W, Zhou J. YAP1/TEAD1 upregulate platelet-derived growth factor receptor beta to promote vascular smooth muscle cell proliferation and neointima formation. J Mol Cell Cardiol. 2021;156:20–32.
32. Misra S, Kilari S, Yang B, Sharma A, Wu CC, Vazquez-Padron RI, Broadwater J. Anti Human CX3CR1 VHH Molecule Attenuates Venous Neointimal Hyperplasia of Arteriovenous Fistula in Mouse Model. J Am Soc Nephrol. 2021;32(7):1630–48.
33. Yan R, Song A, Zhang C. The Pathological Mechanisms and Therapeutic Molecular Targets in Arteriovenous Fistula Dysfunction. Int J Mol Sci. 2024;25(17):9519.
34. Singh AK, Kilari S, Cai C, Misra S. Bindarit encapsulated nanoparticles prevent venous neointimal hyperplasia and restenosis in a murine angioplasty model. Transl Res. 2022;248:68–86.
35. Arteaga EC, Wai C, Uriyanghai U, Rudraraju M, Su H, Sudarsanam VA, Haddad SO, Poulton JS, Roy-Chaudhury P, Xi G. Characterization of Protein Expression and Signaling Pathway Activation That May Contribute to Differential Biological Functions in Porcine Arterial and Venous Smooth Muscle Cells. Int J Mol Sci. 2025;26(7):3110.
36. van Leent MMT, Duivenvoorden R. TGF-β: A Wrench in the Gears of Arteriovenous Fistula Maturation. Arterioscler Thromb Vasc Biol. 2024;44(12):2527–9.
37. Zhang W, Gonzalez L, Li X, Bai H, Li Z, Taniguchi R, Langford J, Ohashi Y, Thaxton C, Aoyagi Y, Yatsula B, Martin KA, Goodwin J, Tellides G, Long X, Shu C, Dardik A. Endothelial TGF-β Signaling Regulates Endothelial-Mesenchymal Transition During Arteriovenous Fistula Remodeling in Mice With Chronic Kidney Disease. Arterioscler Thromb Vasc Biol. 2024;44(12):2509–26.
38. Bezhaeva T, Wong C, de Vries MR, van der Veer EP, van Alem CMA, Que I, Lalai RA, van Zonneveld AJ, Rotmans JI, Quax PHA. Deficiency of TLR4 homologue RP105 aggravates outward remodeling in a murine model of arteriovenous fistula failure. Sci Rep. 2017;7(1):10269.
39. Bezhaeva T, Karper J, Quax PHA, de Vries MR. The Intriguing Role of TLR Accessory Molecules in Cardiovascular Health and Disease. Front Cardiovasc Med. 2022;9:820962.
40. Zhao X, Gu M, Xu X, Wen X, Yang G, Li L, Sheng P, Meng F. CCL3/CCR1 mediates CD14 + CD16- circulating monocyte recruitment in knee osteoarthritis progression. Osteoarthritis Cartilage. 2020;28(5):613–25.
41. Wallace CA, Moir G, Malone DF, Duncan L, Devarajan G, Crane IJ. Regulation of T-lymphocyte CCL3 and CCL4 production by retinal pigment epithelial cells. Invest Ophthalmol Vis Sci. 2013;54(1):722–30.
42. Yuan X, Liu W, Li Y, Chen K, Li H, Tang H, Yin Y, Song Z, Chen D. CCL3 aggravates intestinal damage in NEC by promoting macrophage chemotaxis and M1 macrophage polarization. Pediatr Res.

2023;94(1):119–28.
43. de Jager SC, Bot I, Kraaijeveld AO, Korporaal SJ, Bot M, van Santbrink PJ, van Berkel TJ, Kuiper J, Biessen EA. Leukocyte-specific CCL3 deficiency inhibits atherosclerotic lesion development by affecting neutrophil accumulation. Arterioscler Thromb Vasc Biol. 2013;33(3):e75–83.
44. Mubariki R, Samara R, Gimenez-Arnua AM, Maurer M, Bejar J, Toubi E, Vadasz Z. CD4 + CCR5+ T cells and CCL3 + mast cells are increased in the skin of patients with chronic spontaneous urticaria. Front Immunol. 2024;15:1327040.
45. de Jager SC, Bot I, Kraaijeveld AO, Korporaal SJ, Bot M, van Santbrink PJ, van Berkel TJ, Kuiper J, Biessen EA. Leukocyte-specific CCL3 deficiency inhibits atherosclerotic lesion development by affecting neutrophil accumulation. Arterioscler Thromb Vasc Biol. 2013;33(3):e75–83.
46. Yang YL, Li XF, Song B, Wu S, Wu YY, Huang C, Li J. The Role of CCL3 in the Pathogenesis of Rheumatoid Arthritis. Rheumatol Ther. 2023;10(4):793–808.
47. Liao YY, Tsai HC, Chou PY, Wang SW, Chen HT, Lin YM, Chiang IP, Chang TM, Hsu SK, Chou MC, Tang CH, Fong YC. CCL3 promotes angiogenesis by dysregulation of miR-374b/ VEGF-A axis in human osteosarcoma cells. Oncotarget. 2016;7(4):4310–25.
48. Liu X, Mu L, Ma S, Zhang H. Diagnostic Value of Serum sCD40L, CCL3, and NT-ProBNP Levels in Detection of Lower Limb Venous Thrombosis among Elderly Patients with Heart Failure. Arq Bras Cardiol. 2026;123(1):e20250445.
49. Mir Seyed Nazari P, Marosi C, Moik F, Riedl J, Özer Ö, Berghoff AS, Preusser M, Hainfellner JA, Pabinger I, Zlabinger GJ, Ay C. Low Systemic Levels of Chemokine C-C Motif Ligand 3 (CCL3) are Associated with a High Risk of Venous Thromboembolism in Patients with Glioma. Cancers (Basel). 2019;11(12):2020.
50. Luo X, Zhang N, Liu Y, Du B, Wang X, Zhao T, Liu B, Zhao S, Qiu J, Wang G. Resolving the developmental mechanisms of cardiac microthrombosis of SARS-CoV-2 based on single-cell transcriptome analysis. Sci China Life Sci. 2025;68(1):103–15.
51. Yamashita A, Gi T, Sato Y. Histological differences among thrombi in thrombotic diseases. Curr Opin Hematol. 2025;32(3):146–56.
52. Sun H, Schlamp F, Muller M, Xia Y, Liberow S, Smilowitz NR, Hochman JS, Reynolds HR, Beckman JA, Barrett TJ, Berger JS. Platelets induce endothelial cell mitochondrial dysfunction in myocardial infarction. Sci Adv. 2025;11(46):eadx0268.
53. Zhu Y, Xu W, He Y, Yang W, Song S, Wen C. Therapeutic implications of endoplasmic reticulum stress gene CCL3 in cervical squamous cell carcinoma. Cell Biol Toxicol. 2025;41(1):47.

Figures

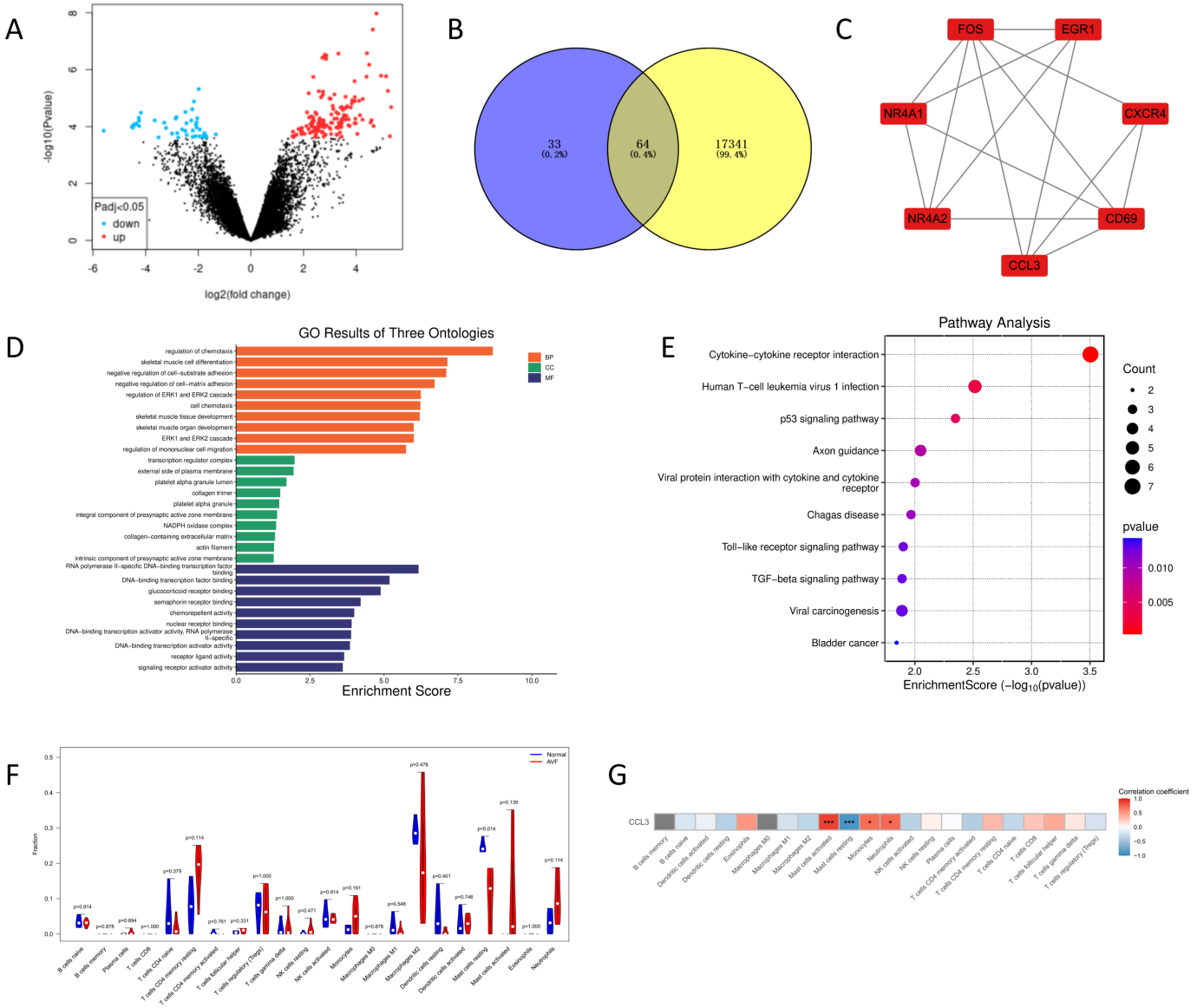


Figure 1

(A)DEGs volcano plot (upregulated genes: 74, downregulated genes: 23).(B) Intersection diagram of DEGs and genes targeting inflammatory responses(Blue indicates DEGs, and yellow denotes inflammation-related targets).(C)Seven core targets.(D)GO results of three ontologies.(E)Pathway Analysis.(F)Differences in the infiltration of various immune cells between the two groups.(G)The correlation between CCL3 and the infiltration of various immune cells.

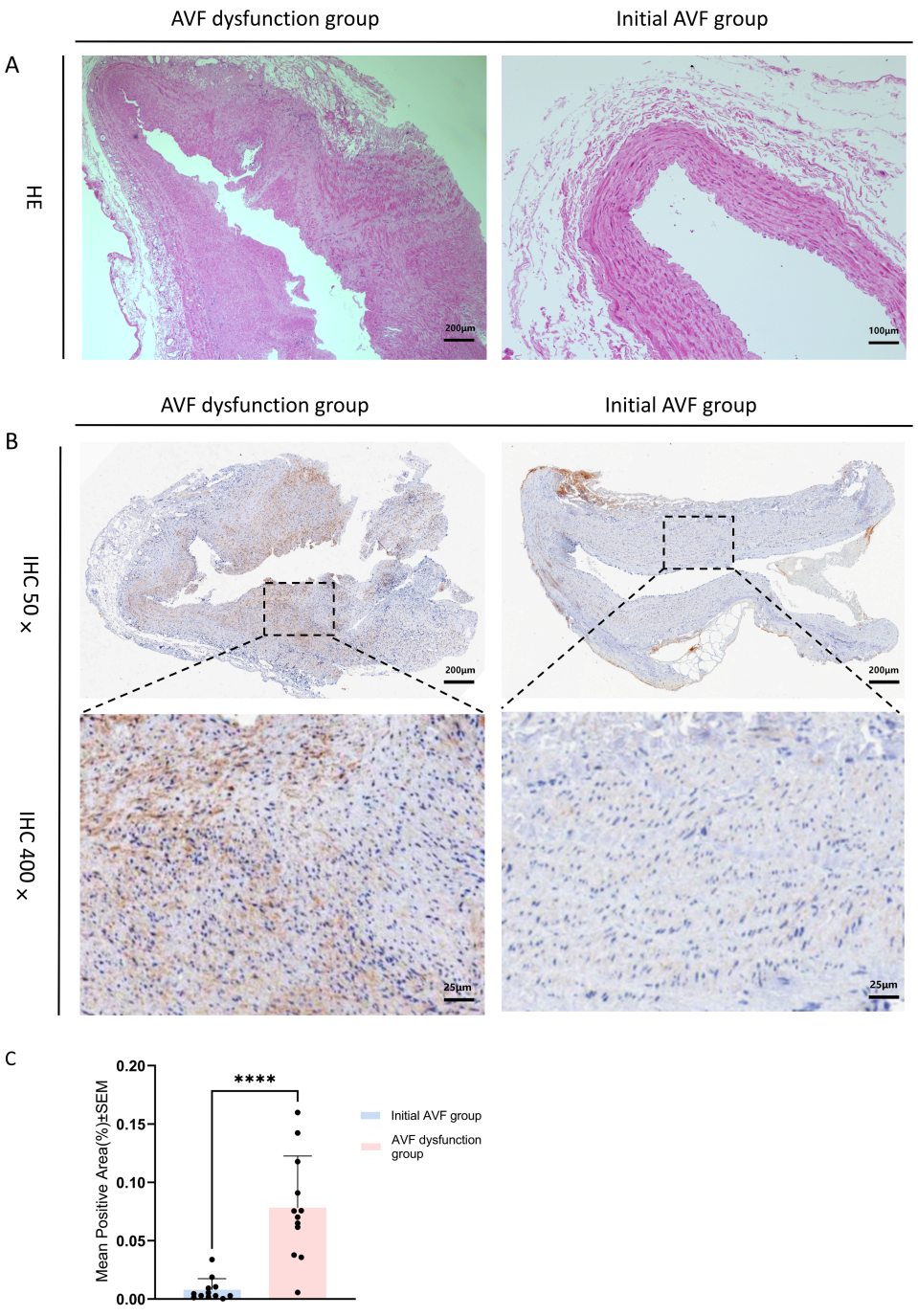


Figure 2

(A)HE staining images. The AVF dysfunction group scale bar is 200μm,the intial AVF group scale bar is 100μm.(B)IHC images.The scale bar is 200μm and 25μm.(C)Relative CCL3 protein expression in the initial AVF and AVF dysfunction groups.